3D Structure of Ramoplanin: A Potent Inhibitor of Bacterial Cell Wall Synthesis[†,‡]

Michael Kurz* and Wolfgang Guba

Central Pharma Research, G838, Hoechst-AG, D-65926 Frankfurt am Main, Germany

Received April 29, 1996; Revised Manuscript Received July 11, 1996[⊗]

ABSTRACT: The 3D structure of ramoplanin was studied by NMR spectroscopy in aqueous solution. A total of 320 interproton distances were determined from a NOESY spectrum and were used as restraints in distance geometry calculations. A structural refinement was carried out by molecular dynamics calculations in a solvent box. The structure of ramoplanin is characterized by two antiparallel β-strands which are formed by the residues 2−7 and 10−14, respectively. The β-strands are connected by six intramolecular hydrogen bonds and a reverse β-turn which is formed by Thr[8] and Phe[9] (in positions i+1 and i+2, respectively). Residues 2 and 14 are connected by a loop consisting of Leu[15], Ala[16], Chp[17], and the side chain of Asn[2]. Although residues 14−17 show the formation of a β-turn, only the N-terminal end of the turn is directly connected to one of the β-strands (Gly[14]), whereas the C-terminal end (Chp[17]) is linked via the side chain of Asn[2]. The 3D conformation of ramoplanin is also stabilized by a hydrophobic cluster of the aromatic sidechains of the residues 3, 9, and 17. This *hydrophobic collapse* leads to a U-shaped topology of the β-sheet with the β-turn at one end and the loop at the other end. The structure found for ramoplanin differs considerably from the published structure of ramoplanose which might be due to a smaller number of NOE distance restraints used in the previous study.

Ramoplanin (also known as A-166686 or MDL 62,198) is a glycolipodepsipeptide antibiotic obtained by fermentation of *Actinoplanes* ATCC 33076 (Cavalleri et al., 1984; Pallanza et al., 1984; Ciabatti et al., 1989a). It has excellent in vitro activity against aerobic and anaerobic Gram-positive bacteria including methicillin-resistant *Staphylococci* (O'Hare et al., 1988, 1990; Maple et al., 1989; Brumfitt et al., 1990) and bacteria resistant to vancomycin, ampicillin, and erythromycin (Pallanza et al., 1984; Ciabatti et al., 1989a; Johnson et al., 1992; Collins et al., 1993). Like β-lactams and glycopeptides, ramoplanin inhibits the cell wall peptidoglycan biosynthesis. In vitro studies by Somner and Reynolds indicated that ramoplanin inhibits the conversion of lipid intermediate I to lipid intermediate II (transfer of *N*-acetylglucosamine) (Somner & Reynolds, 1990; Reynolds & Somner, 1990).

The antibiotic was first isolated as a complex of three closely related components A1, A2, and A3, in which A2 was the most abundant (Cavalleri et al., 1984). The structures of all components were determined mainly on the basis of 2D-NMR spectroscopy (Ciabatti et al., 1989b; Kettenring et al., 1989); the structure of factor A2 is shown in Figure 1. Ramoplanin consists of 17 amino acids in which the C-terminal 3-chloro-4-hydroxyphenylglycine (Chp[17])[1] forms a lactone bond with the hydroxyl group of the β-hydroxyasparagine (β-OH-Asn[2]). The N-terminus of Asn[1] is acylated by three different fatty acids which correspond to the three different components. Two D-mannose moieties are attached to the 4-hydroxyphenylglycine in position 11 (Hpg[11]) by a hemiacetal bond. An antibiotic named ramoplanose or UK-71903 was described by the group of D. H. Williams (Skelton et al., 1991). It contains the same peptide core and differs only by the number of mannose units on Hpg[11] (three instead of two). Other differences described for the configurations of the double bonds in the diunsat-

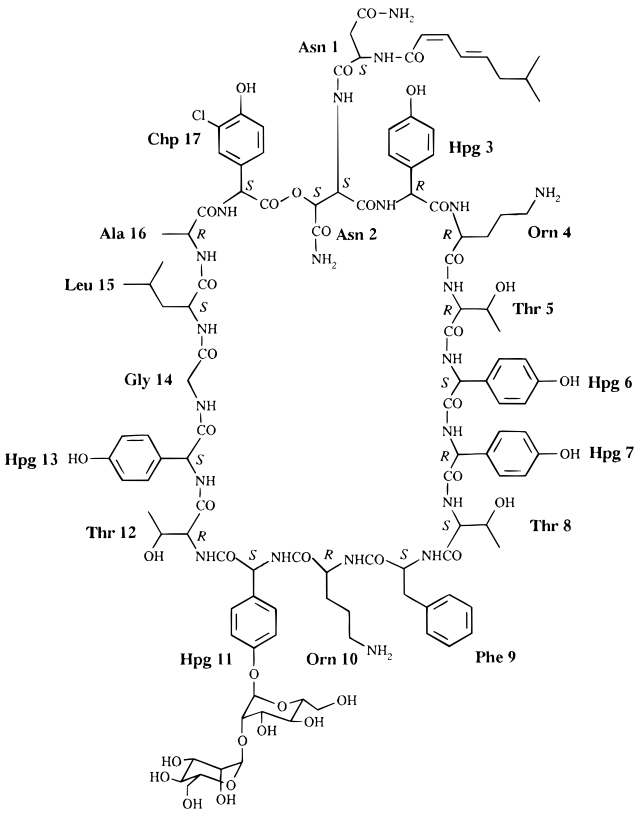

FIGURE 1: Structure of ramoplanin factor A2.

[†] This work was carried out in the Lepetit Research Center, Via R. Lepetit 34, 21040 Gerenzano (VA), Italy.

[‡] The PDB ID code for ramoplanin is 1DSR.

* To whom correspondence should be addressed.

[⊗] Abstract published in *Advance ACS Abstracts,* August 15, 1996.

[1] Abbreviations: 3D, three-dimensional; Chp, chlorohydroxyphenylglycine; DG, distance geometry; DQF-COSY, double-quantum filtered correlated spectroscopy; HMBC, heteronuclear multiple-bond correlation; HMQC, heteronuclear multiple-quantum coherence spectroscopy; Hpg, hydroxyphenylglycine; MD, molecular dynamics; NMR, nuclear magnetic resonance; NOE, nuclear Overhauser effect; NOESY, nuclear Overhauser enhancement spectroscopy; RMS, root mean square; TOCSY, total correlated spectroscopy.

S0006-2960(96)01017-3 CCC: $12.00

urated fatty acid are due to a wrong structure for ramoplanin. The present study clearly shows that the configuration is *cis*,*trans* and therefore identical with the one found for ramoplanose.

The investigation of ramoplanose also included a conformational analysis based on 97 interresidue distance constraints obtained from NOESY spectra, which were used in distance geometry and restrained molecular dynamics calculations. The structure contains two antiparallel β-strands connected by seven intramolecular hydrogen bonds and two reverse turns; one strand incorporates a β-bulge. However, the analysis of NOESY spectra observed for ramoplanin in our laboratory revealed many NOEs which could not be explained by the structure shown for ramoplanose.

Reported in this work is the 3D structure of ramoplanin which was determined by NMR spectroscopy and molecular modeling. It was possible to elucidate one major conformation which is in accordance with all experimentally determined distance restraints including a large number of long-range NOEs. A total of 320 distance constraints were used during these calculations. Compared to the previous studies carried out on ramoplanose, the present investigation gives a new picture about the tertiary structure of the molecule. The significant changes of the 3D structure have important implications for the design of new analogues of ramoplanin with an improved pharmacokinetic profile. This model is also essential for understanding the biological function of ramoplanin, especially the mechanism of interaction with its target enzymes involved in the bacterial cell wall synthesis.

EXPERIMENTAL PROCEDURES

NMR Spectroscopy. All NMR spectra were recorded on a Bruker AMX 600 at 40 °C. 30 mg of ramoplanin-A2 was dissolved in a mixture of H_2O/DMSO-d_6 4:1 (D_2O/DMSO-d_6 4:1, respectively) at pH 4.6. The data were processed on an Aspect station using the UXNMR software from Bruker.

All homonuclear experiments [DQF-COSY (Marion & Wüthrich, 1983), TOCSY (Bax & Davis, 1985), and NOESY (Jeener et al., 1979)] were acquired with spectral widths of 12 ppm. In all experiments, spectra were recorded with 512 increments in t_1 and 4096 complex data points in t_2. For the NOESY 32 transients were averaged for each t_1 value with a relaxation delay of 1.5 s, for COSY and TOCSY 16 transients. Mixing times of 70 and 150 ms were used for TOCSY and NOESY spectra, respectively. Solvent suppression was achieved by a continous irradiation during the recycle delay and during the mixing time of the NOESY spectra recorded in H_2O/DMSO-d_6 and D_2O/DMSO-d_6 to saturate the water signal.

For the HMQC (Bax & Subramanian, 1986) spectrum 512 increments (32 scans) with 2048 complex data points in t_2 were collected using a sweep width of 10 ppm in the proton dimension and 165 ppm in the carbon dimension. A BIRD pulse (Garbow et al., 1982) was applied to suppress magnetization of protons connected to ^{12}C (recovery delay of 200 ms). The HMBC (Bax & Summers, 1986) spectrum was acquired with a sweep width of 12 ppm in the proton and 180 ppm in the carbon dimension. A total of 128 transients were averaged for each of 512 increments in t_1, and 2048 complex points were recorded in t_2. A delay of 3.3 ms was used to suppress $^1J_{CH}$ couplings, and 70 ms were taken for the development of long-range correlations. After Fourier transformation the strong t_1 noise was reduced by a mean row subtraction using the AURELIA program (Bruker).

Molecular Modeling. Distance geometry (DG) calculations, molecular dynamics (MD) simulations, and interactive modeling were performed with DGEOM95 (Blaney et al., 1990), DISCOVER (Consistent Valence Force Field), and INSIGHT II from Biosym Technologies (San Diego, CA) and Tripos' Sybyl Version 6.1a on SGI 340/VGX, SGI ONYX, and Cray YMP computers. The cyclic starting structure was modeled manually with an arbitrary selection of configurations (*R*/*S*) for the stereogenic centers of Hpg^6 and Hpg^7.

With DGEOM95, structures were generated from the NMR-derived distance constraints with floating chirality for the above-mentioned stereogenic centers. The 320 interproton distances for the generation of the distance matrix were obtained by volume integration of the NOESY spectra in H_2O/DMSO-d_6 and D_2O/DMSO-d_6, respectively. The distance of 1.78 Å between the geminal Hα protons of Gly^{14} was used for calibration. A tolerance of 10% and the usual pseudoatom corrections were applied. The maximum allowed distance violation was 0.7 Å.

The five structures with the lowest restraint energy violations were very similar (average RMS deviation for the superposition of backbone atoms: 0.7 Å) and, therefore, the structure with the minimum restraint violation energy was selected for a further conformational refinement by molecular dynamics taking into account electrostatics and solvent effects. For this purpose, the structure was placed into an H_2O solvent box ($x = y = z = 40$ Å; 1966 H_2O molecules) applying the SPC water model (Berendsen et al., 1981). The geometric mean was used for the Lennard-Jones parameters between unlike atoms. Neighbor lists for the calculation of nonbonded interactions were updated within a radius of 14 Å. The actual calculation of nonbonded interactions was carried out up to a radius of 12 Å without the use of switching functions. For all the MD simulations three-dimensional periodic boundary conditions and a time step of 1 fs were employed. Throughout the MD simulation, temperature and pressure (1.0 bar) bath coupling (Berendsen et al., 1984) was applied.

The simulation protocol was as follows: while the solute was fixed, the solvent was energy-minimized for 2000 iterations by conjugate gradients with a convergence criterion of 1 kcal/Å. The solvent shell was further relaxed by a 10 ps MD simulation at a temperature of 310 K (constant volume). After removing the fixed atom constraints the NMR-derived distance restraints were applied with a maximum force of 1000 kcal $Å^{-1}$ mol^{-1}, the system was minimized for 20 000 iterations by conjugate gradients with a convergence criterion of 1 kcal/Å and then gradually heated from 50 to 250 K in 50 K steps for 1 ps each. The system was equilibrated at 313 K for 50 ps, after then the trajectory was sampled at 313 K in 1 ps intervals for 450 ps. The MD calculation was resumed for another 500 ps without distance restraints. The remaining simulation parameters were kept unchanged. From the trajectories of both the restrained and the free MD simulations, six frames in 75 ps intervals, respectively, were energy-minimized *in vacuo* with 200-step conjugate gradients and a distance-dependent dielectric constant.

Table 1: Proton Chemical Shifts, J(HN−HC$^{\alpha}$) Coupling Constants, and Amide Proton Temperature Coefficients of Ramoplanin[a,b]

residue	HN	HC$^{\alpha}$	HC$^{\beta}$	others	J(HN−HC$^{\alpha}$) (Hz)	$\Delta\delta/T$ (−ppb K^{-1})
Asn[1]	8.09	4.74	2.24/1.71	−	7.6	6.6
Asn[2]	8.42	5.53	5.76	amides 6.60/6.20	9.7	1.8
Hpg[3]	9.86	6.28	−	b/f 7.56, c/e 7.08	8.8	5.7
Orn[4]	9.24	4.28	1.45/1.27	HC$^{\gamma}$ 1.26, HC$^{\delta}$ 2.68/2.47	7.9	2.8
Thr[5]	7.58	4.39	4.1	HC$^{\gamma}$ 1.15	6.5	3.5
Hpg[6]	8.9	6.82	−	b/f 6.75, c/e 6.41	9.7	7.1
Hpg[7]	8.95	5.48	−	b/f 6.72, c/e 6.52	5.0	4.7
Thr[8]	8.26	3.76	3.95	HC$^{\gamma}$ 0.77	2.9	6.7
Phe[9]	7.59	4.2	2.19/1.93	b/f 6.99, c/e 7.28, d 7.22	6.5	4.2
Orn[10]	7.77	5.03	2.14/2.06	HC$^{\gamma}$ 1.77, HC$^{\delta}$ 3.10/3.05	9.1	2.4
Hpg[11]	9.27	6.98	−	b/f 7.40, c/e 6.97	7.9	5.5
Thr[12]	9.11	4.76	3.97	HC$^{\gamma}$ 0.99	9.1	4.3
Hpg[13]	8.85	6.11	−	b/f 7.13, c/e 6.78	5.3	4.9
Gly[14]	7.92	3.80/3.03	−	−	−	1.5
Leu[15]	8.36	4.31	1.53	HC$^{\gamma}$ 1.53, HC$^{\delta}$ 0.81/0.77	2.9	6.2
Ala[16]	9.29	4.36	1.46	−	5.5	6.6
Chp[17]	7.94	4.92	−	b 6.45, e 6.93, f 6.63	9.7	2.5

[a] In H_2O/DMSO-d_6 (4:1) at pH 4.6, 40 °C. Referenced to TMS. The resonances of the mannose moieties could not be assigned completely due to spectral overlap. [b] 7-Methylocta-2,4-dienoyl residue: HC$^{\alpha}$ 5.59, HC$^{\beta}$ 6.51, HC$^{\gamma}$ 7.14, HC$^{\delta}$ 6.10, HC$^{\epsilon}$ 2.06/1.99, HC$^{\zeta}$ 1.50, CH_3 0.87.

Table 2: Carbon Chemical Shifts of Ramoplanin[a,b]

residue	C$^{\alpha}$	C$^{\beta}$	others
Asn[1]	51.1	38.2	−
Asn[2]	53.6	73.8	−
Hpg[3]	56.9	−	a 130.6, b/f 130.6, c/e 117.5, d 157.0
Orn[4]	55.0	29.2	C$^{\gamma}$ 24.3, C$^{\delta}$ 40.1
Thr[5]	59.1	69.5	C$^{\gamma}$ 21.0
Hpg[6]	55.4	−	a 130.4, b/f 129.3, c/e 116.2, d 156.7
Hpg[7]	58.3	−	a,[c] b/f 128.8, c/e 116.8, d 157.1
Thr[8]	63.7	66.6	C$^{\gamma}$ 19.0
Phe[9]	57.9	37.6	a,[c] b/f 130.1, c/e 130.0, d 128.3
Orn[10]	52.7	31.5	C$^{\gamma}$ 24.7, C$^{\delta}$ 40.5
Hpg[11]	56.3	−	a 132.8, b/f 128.3, c/e 118.4, d 157.4
Thr[12]	59.3	69.8	C$^{\gamma}$ 21.1
Hpg[13]	56.7	−	a 131.2, b/f 129.4, c/e 117.0, d 157.3
Gly[14]	43.9	−	−
Leu[15]	54.6	40.3	C$^{\gamma}$ 25.6, C$^{\delta}$ 23.3, C$^{\delta'}$ 23.3
Ala[16]	51.4	17.6	−
Chp[17]	54.3	−	a,[c] b 128.3, c 127.5, d 153.0, e 118.1, f 127.9

[a] In H_2O/DMSO-d_6 (4:1) at pH 4.6, 40 °C. Referenced to DMSO-d_6 at 39.5 ppm. [b] 7-Methylocta-2,4-dienoyl residue: C$^{\alpha}$ 118.5, C$^{\beta}$ 144.1, C$^{\gamma}$ 128.8, C$^{\delta}$ 145.7, C$^{\epsilon}$ 43.2, C$^{\zeta}$ 29.4, CH_3 23.4. [c] Not determined due to spectral overlap.

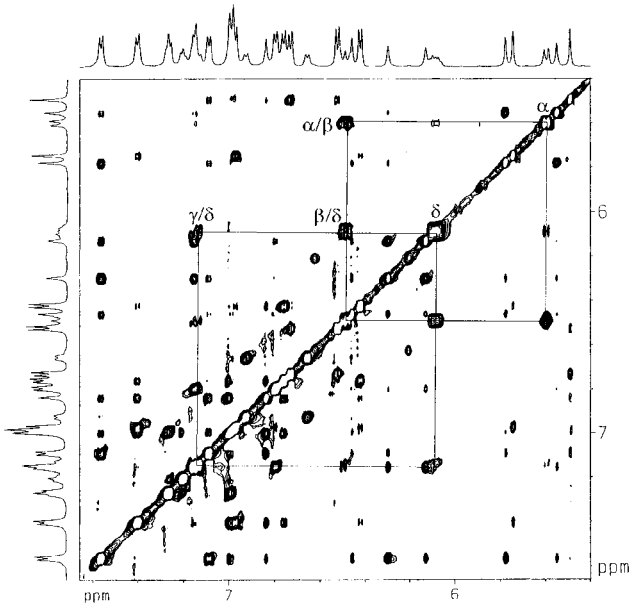

FIGURE 2: Region of the NOESY spectrum of ramoplanin in D_2O/DMSO-d_6 4:1 at pH 4.6, 40 °C (mixing time 150 ms). The spin system of the olefinic protons of the fatty acid chain is indicated. The intense NOE between Hβ and Hδ proves the *trans*-configuration of the second double bond.

RESULTS

The NMR analysis was carried out under the same conditions (H_2O/DMSO-d_6 4:1 at pH 4.6, 40 °C) which were found by Kettenring et al. (1989) to exhibit well-resolved resonances of narrow line width. All proton and most of the carbon resonances were assigned using DQF-COSY, TOCSY, NOESY, HMQC, and HMBC spectra. The proton chemical shifts are reported in Table 1, and most of them are in accordance with the data previously reported (Kettenring et al., 1989). Only the chemical shifts of the amide and α-protons of Phe[9] and Orn[10] were obviously interchanged. The carbon chemial shifts are reported in Table 2. Due to spectral overlap, the carbonyl carbons and some of the aromatic carbons could not be assigned unambiguously.

A careful inspection of the NOESY spectum recorded in D_2O/DMSO-d_6 revealed that the configuration of the second double bond in the fatty acid chain had to be revised with respect to the previously published structure (Kettenring et al., 1989). As in the case of ramoplanose (Skelton et al., 1991) this double bond is *trans*-configured, which was proved by an intense NOE between Hβ and Hδ and a relatively weak NOE between Hγ and Hδ (see Figure 2).

Figure 1 of the supporting information shows the NOESY spectrum of ramoplanin-A2 in H_2O/DMSO-d_6 recorded with a mixing time of 150 ms. The quantitative analysis resulted in 320 interproton distances, which were used in the later molecular modeling calculations (a list of all NOEs is available as supporting information). An analysis of the distribution of the NOEs is given in Figure 3. From 320 NOEs, 61 are intraresidual, 112 are between protons from residue i to i+1, 19 from i to i+2, and 128 from i to i+x, with $x \geq 3$ (protons of the fatty acid were formally assigned to residue 1). A similar analysis of the NOEs reported for ramoplanose (Skelton et al., 1991) reveals two "intraresidue" NOEs (Hpg[11]3,5/mannose[11] and Asn[1]NH/F2, with F2 belonging to the fatty acid side chain), 56 from i to i+1, five from i to i+2, and 34 from i to i+x, with $x \geq 3$ [the NOE

	1	2	3	4	5	6	7	8	9	10	11	12	13	14	15	16	17
1	10	6											6	2	8	5	1
2	6	3	9										1	2	1	3	4
3		9	3	6		1	2	1	4	2		3	6	2			5
4			6	3	9						1	5	11				1
5				9	3	11					3	7					
6			1		11	2	3			11	7	4					
7			2			3	2	8	2	5							
8			1				8	3	8	4							
9			4					8	8	6						1	11
10			2			11	5	4	6	4	10						
11				1	3	7				10	1	7	1				
12			3	5	7	4					7	4	8				
13	6	1	6	11							1	8	1	7	5		
14	2	2	2										7	2	3		3
15	8	1											5	3	5	4	6
16	2	5							1						4	0	7
17	1	4	5						11					3	6	7	7

FIGURE 3: Distribution of NOEs between the different residues in ramoplanin. A high number of long-range NOEs are observed, especially between Phe[9]and Chp[17], between Orn[4] and Hpg[13], and between Hpg[6] and Orn[10].

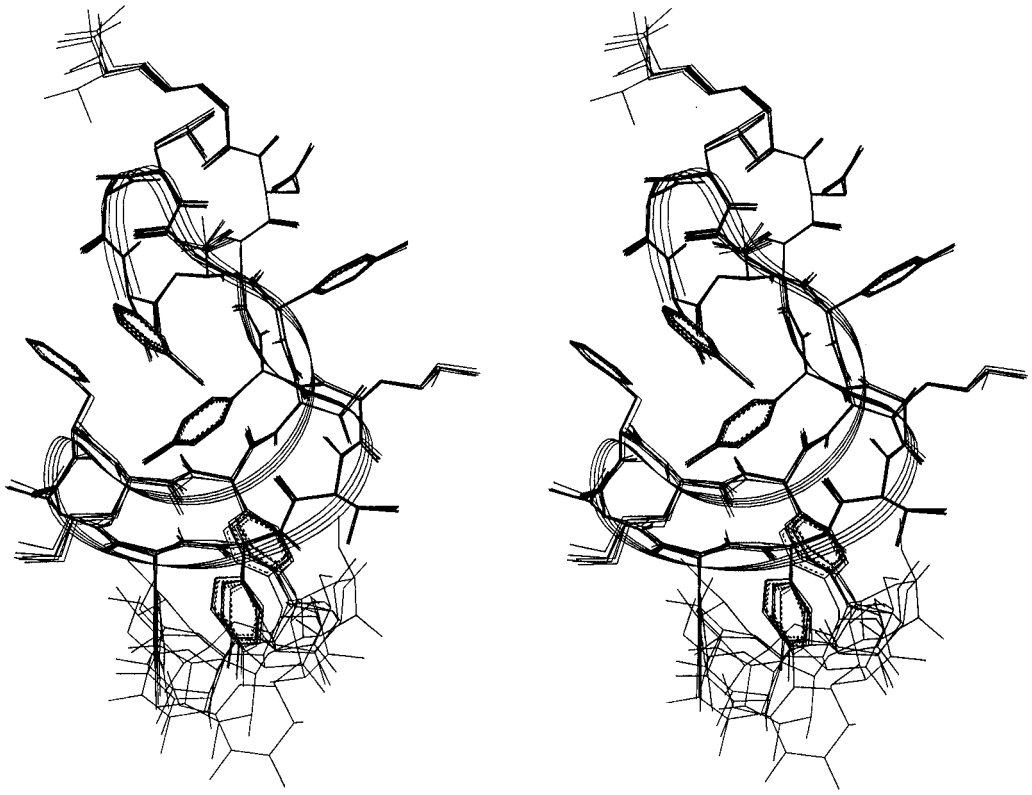

FIGURE 4: Stereopresentation of the superposition of six structures of ramoplanin obtained during the restrained MD simulation in 75 ps intervals.

table in Skelton et al. (1991) contains 98 NOEs, three of them are listed twice. By counting NOEs to F8/F8′ as two NOEs the total number is, in fact, 97].

The high number of long-range NOEs clearly indicates a well-defined 3D structure for ramoplanin in aqueous solution. The highest numbers of interresidual NOEs, namely, 11, are observed between Phe[9] and Chp[17], between Orn[4] and Hpg[13], and between Hpg[6] and Orn[10] (for ramoplanose five NOEs were reported between Orn[4] and Hpg[13], but no NOEs were reported for the two remaining pairs of residues).

The interproton distances for ramoplanin were obtained by integration of the NOESY spectra in H_2O/DMSO-d_6 and D_2O/DMSO-d_6, respectively (both spectra were recorded with a mixing time of 150 ms). The cross-peaks observed

Table 3: Backbone Dihedral Angles of Ramoplanin (in deg)[a,b]

residue	ϕ	ψ	ω
Asn[1]	−70 (9)	109 (13)	170 (8)
Asn[2]	−105 (13)	153 (8)	175 (6)
Hpg[3]	140 (9)	−104 (11)	−172 (7)
Orn[4]	70 (12)	52 (9)	−175 (7)
Thr[5]	128 (12)	−150 (10)	−170 (7)
Hpg[6]	−109 (14)	159 (9)	160 (10)
Hpg[7]	169 (8)	−130 (11)	178 (7)
Thr[8]	−56 (12)	−50 (9)	178 (6)
Phe[9]	−77 (11)	−20 (12)	177 (8)
Orn[10]	132 (14)	−134 (14)	−170 (7)
Hpg[11]	−142 (13)	120 (12)	174 (7)
Thr[12]	122 (13)	−121 (9)	180 (8)
Hpg[13]	−153 (9)	123 (12)	−160 (9)
Gly[14]	−152 (13)	46 (15)	160 (8)
Leu[15]	61 (11)	81 (10)	−164 (5)
Ala[16]	82 (11)	6 (12)	168 (7)
Chp[17]	−88 (12)	−21 (14)	

[a] Chp[17]α−Chp[17]C′−Chp[17]O−AsnC$^{\beta}$: −170 (10). Chp[17]C′−Chp[17]O−Asn[2]C$^{\beta}$−Asn[2]C$^{\alpha}$: 111 (19). Chp[17]O−Asn[2]C$^{\beta}$−Asn[2]C$^{\alpha}$−Asn[2]C′: −70 (5). [b] The dihedral angles (deg) are the average values over a trajectory of 450 ps restrained MD. The standard deviation is given in parentheses.

Table 4: Intramolecular Hydrogen Bonds in Ramoplanin[a]

donor	acceptor	average distance
Orn[4]−NH	Thr[12]−CO	1.91 (0.14)
Thr[5]−NH	Thr[12]−CO	2.87 (0.20)
Hpg[7]−NH	Orn[10]−CO	2.20 (0.21)
Orn[10]−NH	Hpg[7]−CO	2.86 (0.34)
Thr[12]−NH	Thr[5]−CO	2.18 (0.20)
Gly[14]−NH	Asn[2]−CO	2.37 (0.20)
Ala[16]−NH	FA−CO	1.94 (0.15)

[a] The distances (Å) are the average values over a trajectory of 450 ps restrained MD. The standard deviation is given in parentheses.

between the geminal Hα protons of Gly[14] were used for calibration by setting the corresponding distance to 1.78 Å.

A direct comparison with the data obtained for ramoplanose is limited because in this case only a classification into "small", "medium", and "large" NOEs was given. From 24 NOEs which were classified as "medium" and which were also found in our study of ramoplanin, 11 corresponding interproton distances were shorter than 2.5 Å, six were between 2.5 and 3.0 Å, and seven were longer than 3.0 Å. From NOEs classified as "small" we found two corresponding distances, namely, Asn[2]-NH/Asn[1]α and Ala[16]-NH/Chp[17]-NH, to be 2.2 and 2.4 Å, respectively. Another 10 "small" NOEs correspond to distances between 2.5 and 3.0 Å in ramoplanin, and 29 correspond to distances longer than 3.0 Å. The remaining 30 NOEs in Table III from Skelton et al. (1991) were either not present in the NOESY spectra of ramoplanin or could not be assigned unambiguously due to spectral overlap. Some of the differences between our results and those obtained for ramoplanose might be due to spin diffusion during the long mixing times of 400 and 250 ms which were used by Williams and his co-workers (Skelton et al., 1991).

DISCUSSION

The configurations of all amino acids except Hpg[6] and Hpg[7] were previously determined by GC−MS analysis on a chiral column (Ciabatti et al., 1989b). Therefore, the distance geometry calculations were carried out with floating chirality for these two stereogenic centers. In the five structures with the lowest restraint energy violation, the configuration of Hpg[6] is *S* whereas the one of Hpg[7] is *R*. This is in accordance with the chirality pattern obtained for ramoplanose by chiral GC−MS and NOE analysis (Skelton et al., 1991).

As can be seen from the superposition of six structures (Figure 4), the 3D conformation of ramoplanin is very well maintained throughout the restrained MD simulation. This is supported by the averaged backbone dihedral angles and the corresponding standard deviations given in Table 3. Only the sugar substituents of residue 11 display a high degree of conformational flexibility because of the low number of NOE restraints in this part of the molecule. The structure of ramoplanin is characterized by two antiparallel β-strands which are formed by the residues 2−7 and 10−14, respectively. The β-strands are connected by six intramolecular hydrogen bonds (see Table 4) and a reverse β-turn which is formed by Thr[8] and Phe[9] (in positions i+1 and i+2, respectively). The φ and ψ dihedral angles of these residues

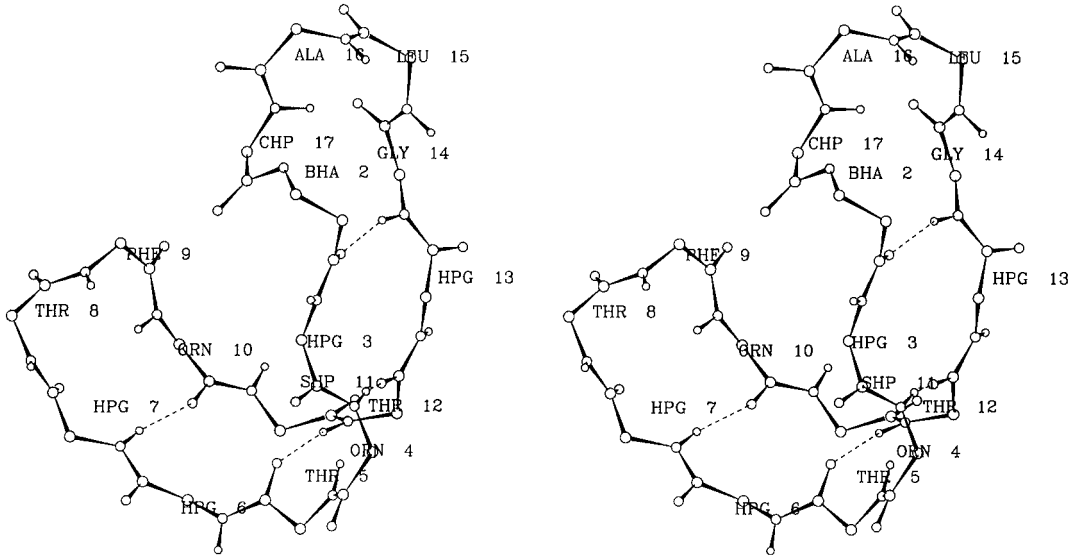

FIGURE 5: Stereopresentation of the β-sheet indicating the intramolecular hydrogen bonds. For the sake of clarity, the side chains of the amino acids are represented only by the C$^{\beta}$-carbons. BHA 2 corresponds to the β-hydroxyasparagine Asn[2], and SHP 11 corresponds to Hpg[11].

(Table 3) correspond to the values of a βI-turn, which is the expected turn conformation for two L-amino acids in positions $i+1$ and $i+2$ (Smith & Pease, 1980).

It should be pointed out that the corresponding hydrogen bond between the amide proton of Orn[10] and the carbonyl oxygen of Hpg[7] is not very well defined during the simulation (see Table 4). However, a ^{1}H-spectrum recorded in D_2O/DMSO-d_6 immediately after sample preparation reveals that the amide proton of Orn[10] is in slow exchange with the solvent (Figure 2 of the supporting information). The same is true for the amide protons of Thr[5], Hpg[7], Thr[12], and Gly[14] supporting in all cases the presence of an intramolecular hydrogen bond. Only in the case of Orn[4] is the exchange rate not in accordance with the formation of a hydrogen bond.

Residues 2 and 14 are connected by a loop consisting of Leu[15], Ala[16], Chp[17], and the side chain of Asn[2]. Although residues 14−17 show the formation of a β-turn, only the N-terminal end of the turn is directly connected to a β-strand (Gly[14]) whereas the C-terminal end (Chp[17]) is linked via the side chain of Asn[2]. The slow exchange observed for the amide proton of Chp[17] would correspond to the formation of a hydrogen bond to the carbonyl oxygen of Gly[14]. However, during the MD simulation this hydrogen bond is only partially populated (average distance NH−CO = 3.2 Å). The slow exchange rate observed for the amide proton of Asn[2] cannot be explained by the formation of an intramolecular hydrogen bond; instead a poor solvent accessibility due to sterical shielding must be assumed. The 3D conformation of ramoplanin is also stabilized by a hydrophobic cluster of the aromatic sidechains of the residues 3, 9, and 17. This "hydrophobic collapse" (Wiley & Rich, 1993) prevents water molecules from entering the concave side of the molecule and, thus, promotes the formation of internal hydrogen bonds.

In contrast to the structure given for ramoplanose, the lactone linkage between Asn[2] and Chp[17] adopts a trans conformation. The main difference, however, between the structure proposed for ramoplanose and the structure of ramoplanin is that the overall topology of the β-sheet is U-shaped with the β-turn at one end and the loop at the other end (Figure 5). In the case of ramoplanose, the β-sheet obtains a much more planar structure. The differences between ramoplanose and ramoplanin are probably caused by the relatively small number of restraints used in the earlier study. Due to the computational limitations in their study only a subset of the 97 interproton distances, namely, those between amide NH, C_αH, and C_βH protons, were included. This left a number of 35 restraints, and only 11 of them were long-range correlations between residues i and $i+x$ with $x \geq 2$.

During the free MD simulation the overall topology of ramoplanin was maintained, but secondary structural elements, such as intramolecular hydrogen bonds, which are in accordance with experimental findings, started to loosen up because of the formation of hydrogen bonds with the surrounding water molecules. In contrast to MD simulations of large proteins, where the 3D structure is stabilized by numerous intramolecular interactions, secondary structure elements of small- and medium-sized peptides in force field calculations must be stabilized by adding NMR-derived distance restraints.

SUPPORTING INFORMATION AVAILABLE

A list of the 320 NMR-derived distance restraints in comparison with the corresponding interproton distances during the MD trajectory is available. In addition, the NOESY spectrum of ramoplanin in H_2O/DMSO-d_6 4:1 at pH 4.6, 40 °C (Figure 1) and a presentation of the amide region of the ^{1}H-spectrum of ramoplanin in H_2O/DMSO-d_6 4:1 at pH 4.6, 40 °C and in D_2O/DMSO-d_6 4:1 at pH 4.6, 40 °C (Figure 2) are availbable (16 pages). Ordering information is given on any current masthead page.

REFERENCES

Bax, A., & Davis, D. G. (1985) *J. Magn. Reson.* 355−360.

Bax, A., & Subramanian, S. (1986) *J. Magn. Reson. 67*, 565−569.

Bax, A., & Summers, M. F. (1986) *J. Am. Chem. Soc. 108*, 2093−2094.

Berendsen, H. J. C., Postma, J. P. M., & van Gunsteren, Hermans J. (1981) *Intermolecular Forces* (Pullman, B., Ed.) Reidel, Dordrecht, The Netherlands.

Berendsen, H. J. C., Postma, J. P. M., van Gunsteren, W. F., DiNola, A., & Haak, J. R. (1984) *J. Chem. Phys. 81*, 3684−3690.

Blaney, J. M., Crippen, G. M., Dearing, A., & Dixon, S. (1990) *DGEOM*, Quantum Chemistry Program Exchange, No. 590, Indiana University, Bloomington, IN.

Brumfitt, W., Maple, P. A. C., & Hamilton-Miller, J. M. T. (1990) *Drugs Exp. Clin. Res. 16*, 377−383.

Cavalleri, B., Pagani, H., Volpe, G., Selva, E., & Parenti, F. (1984) *J. Antibiot. 37*, 309−317.

Ciabatti, R., & Cavalleri, B. (1989a) *Progress in Industrial Microbiology: Bioactive Metabolites from Microorganisms* (Bushell, M. E., & Graefe, U., Eds.) Vol. 27, pp 205−219, Elsevier, New York.

Ciabatti, R., Kettenring, J. K., Winters, G., Tuan, G., Zerilli, L., & Cavalleri, B. (1989b) *J. Antibiot. 42*, 254−267.

Collins, L. A., Eliopoulos, G. M., Wennerstein, C. B., Ferraro, M. J., & Moellering, R. C., Jr. (1993) *Antimicrob. Agents Chemother. 37*, 1364−1366.

Garbow, J. R., Weitkamp, D. P., & Pines, A. (1982) *Chem. Phys. Lett. 93*, 504−509.

Jeener, J., Meier, H., Bachmann, P., & Ernst, R. R. (1979) *J. Chem. Phys. 71*, 4546−4553.

Johnson C. C., Taylor, S., Pitsakis, P., May, P., & Levison, M. E. (1992) *J. Antimicrob. Chemother. 36*, 2342−2345.

Kettenring, J. K., Ciabatti, R., Winters, G., Tamborini, G., & Cavalleri, B. (1989) *J. Antibiot. 42*, 268−275.

Maple, P. A. C., Hamilton-Miller, J. M. T., & Brumfitt, W. (1989) *J. Antimicrob. Chemother. 23*, 517−525

Marion, D., & Wüthrich, K. (1983) *Biochem. Biophys. Res. Commun. 113*, 967−974.

O'Hare, M. D., Felmingham, D., & Grüneberg, R. N. (1988) *Drugs Exp. Clin. Res. 14*, 617−619.

O'Hare, M. D., Ghosh, G., Felmingham, D., & Grüneberg, R. N. (1990) *J. Antimicrob. Chemother. 25*, 217−220.

Pallanza, R., Berti, M., Scotti, R., Randisi, E., & Arioli, V. (1984) *J. Antibiot. 37*, 318−324.

Reynolds, P. E., & Somner, E. A. (1990) *Drugs Exp. Clin. Res. 16*, 385−389.

Skelton, N. J., Harding, M. M., Mortishire-Smith, R. J., Rahman, S. K., Williams, D. H., Rance, M. J., Ruddock, J. C. (1991) *J. Am. Chem. Soc. 113*, 7522−7530.

Smith, J. A., & Pease,L. G. (1980) *CRC Crit. Rev. Biochem.* 315−399.

Somner, E. A., & Reynolds, P. E. (1990) *Antimicrob. Agents Chemother. 34*, 413−419.

Rance M. J., & Ruddock, J. C. (1991) *J. Am. Chem. Soc. 113*, 7522−7530.

Wiley, R. A., & Rich, D. (1993) *Med. Res. Rev.* 3, 327−384.

BI961017Q